A Bayesian Model of the DNA Barcode Gap

Jarrett D. Phillips[1,2]* (ORCID: 0000-0001-8390-386X)

[1]*School of Computer Science, University of Guelph, Guelph, ON., Canada, N1G2W1*

[2]*Department of Integrative Biology, University of Guelph, Guelph, ON., Canada, N1G2W1*

*Corresponding Author: Jarrett D. Phillips[1]

Email Address: jphill01@uoguelph.ca

Running Title: Bayesian inference for DNA Barcode Gap Estimation

<center>**Abstract**</center>

Keywords: Bayesian inference, DNA barcoding, intraspecific genetic distance, interspecific genetic distance, specimen identification, species discovery, Stan

1   Introduction

Since its inception over 20 years ago, DNA barcoding (Hebert et al., 2003a,b) has emerged as a robust method of specimen identification and species delimitation across myriad taxonomic groups which have been sequenced at short, standardized gene regions like 5'-COI for animals. However, the success of the approach, particularly for regulatory and forensic applications, depends crucially on two important factors: (1) the availability of high-quality specimen records found in public reference sequence databases such as the Barcode of Life Data Systems (BOLD) (Ratnasingham and Hebert, 2007), and (2) the establishment of a DNA barcode gap — the idea that the maximum genetic distance observed within species is much smaller than the minimum degree of marker variation found among species (Meyer and Paulay, 2005; Meier et al., 2008). Early work has demonstrated that the presence of a DNA barcode gap hinges strongly on extant levels of species haplotype diversity gauged from comprehensive specimen sampling at wide geographic and ecological scales (Bergsten et al., 2012). Despite this, many taxa lack adequate separation in their pairwise intraspecific and interspecific genetic distances, thereby compromising rapid matching of unknown samples to expertly-validated references, and leading to cases of false positives (taxon oversplitting) and false negatives (excessive lumping of taxa) as a result of incomplete lineage sorting/retention of ancestral polymorphisms, hybridization/introgression, species synonymy, cryptic species diversity, and misidentifications (Hubert and Hanner, 2015; Phillips et al., 2022).

Recent work has argued that DNA barcoding, in its current form, is lacking in statistical rigor, as most studies rely strongly on heuristic distance-based measures to infer taxonomic identity, and of these studies, few report measures of uncertainty, such as standard errors (SEs) and confidence intervals (CIs), around estimates of intraspecific and interspecific variation, calling into question the existence of a true species' DNA barcode gap (Phillips et al., 2022). To support this notion, novel nonparametric locus-specific metrics based on the multispecies coalescent (Rannala and Yang, 2003; Yang and Rannala, 2017) were recently outlined and shown to hold strong promise when applied to predatory *Agabus* (Coleoptera: Dytiscidae) diving beetles (Phillips et al., 2024), a group, which, despite their morphological uniformity, is widely considered to be a taxonomic nightmare (Bergsten et al., 2012). Further, the metrics indicate that sister species pairs from this taxon are often difficult to distinguish on the basis of their DNA barcode sequences (Phillips et al., 2024). Using sequence data from three mitochondrial markers (5'-COI, 3'-COI, and CYTB) obtained from BOLD and GenBank, results highlight that DNA barcoding has been one-sided: there is a need to balance both the sufficient collection of specimens, as well as the deep sampling of species (Phillips et al., 2024). DNA barcode libraries are biased toward the latter. The coalescent (Kingman, 1982) encompasses a backwards continuous-time stochastic Markov process of allelic sampling within natural, neutrally-evolving, species populations towards the Most

<center>2</center>

Recent Common Ancestor (MRCA). The estimators represent a "middle gound" between simple, yet arbitrary, heuristics such as the 2% rule (Hebert et al., 2003a) and the $10\times$ rule (Hebert et al., 2004) and quantify the extent of asymmetric directionality of proportional genetic distance distribution overlap/separation for species within well-sampled taxonomic genera based on a straightforward distance count. The metrics can be employed in a variety of ways, including to assess performance of marker genes for species identification (as in Phillips et al. (2024)), as well as to assess whether computed values are consistent with population genetic-level parameters like effective population size (N_e), mutation rates (μ) and divergence times (τ) for species under study (Mather et al., 2019). However, what appears to be missing is a rigorous statistical treatment of the DNA barcode gap, along an unbiased way to compute the statistical accuracy of the recommended estimators arising through problems inherent in frequentist maximum likelihood estimation for probability distributions having bounded positive support on the closed unit interval [0, 1]. To this end, here, a Bayesian model of the DNA barcode gap coalescent is introduced to rectify such issues. The model allows accurate estimation of posterior means, posterior standard deviations (SDs), posterior quantiles, and credible intervals (CrIs) for the metrics given datasets of intraspecific and interspecific genetic distances for species of interest.

2 Methods

2.1 DNA Barcode Gap Metrics

Recently, Phillips et al. (2024) proposed novel nonparametric maximum likelihood estimators (MLEs) of proportional overlap/separation between intraspecific and interspecific pairwise genetic distance distributions for a given species (x) to aid assessment of the DNA barcode gap as follows:

$$p_x = \frac{\#\{d_{ij} \geq a\}}{\#\{d_{ij}\}} \tag{1}$$

$$q_x = \frac{\#\{d_{XY} \leq b\}}{\#\{d_{XY}\}} \tag{2}$$

$$p'_x = \frac{\#\{d_{ij} \geq a'\}}{\#\{d_{ij}\}} \tag{3}$$

$$q'_x = \frac{\#\{d'_{XY} \leq b\}}{\#\{d'_{XY}\}} \tag{4}$$

where d_{ij} are pairwise genetic distances within species, d_{XY} are genetic distances among species for an entire genus of concern, and d'_{XY} are combined interspecific distances for a target species and its closest neighbouring species. The notation # reflects a count. Quantities a, a', and b correspond to $\min(d_{XY})$, $\min(d'_{XY})$, and $\max(d_{ij})$, the minimum interspecific distance, and the maximum intraspecific distance, respectively (**Figure 1**). Hence, Equations (1)-(4) are simply empirical means of genetic distances falling at and below, or at and exceeding given distribution thresholds. Notice further that a/a', and b

are also the first and nth order statistics, $X_{(1)}$ and $X_{(n)}$, respectively. Equations (1)-(4) can be also be expressed in terms of empirical cumulative distribution functions (ECDFs) (see **Supplementary Information** for details). Genetic distances are easily computed from a model of DNA sequence evolution, such as uncorrected or corrected p-distances (Jukes and Cantor, 1969; Kimura, 1980). If a focal species is found to have multiple nearest neighbours, then the species possessing the smallest average pairwise interspecific distance is used. While these schemes differ considerably from the usual definition of the DNA barcode gap laid out by Meyer and Paulay (2005) and Meier et al. (2008), they more accurately account for species' coalescence histories inferred from contemporaneous samples of DNA sequences, such as interspecific hybridization/introgression events (Phillips et al., 2024). Note, genetic distances are constrained to the unit interval [0, 1], whereas the metrics are defined only on $[a/a', b]$. Values of the estimators obtained from equations (1)-(4) close to or equal to zero give evidence for separation between intraspecific and interspecific genetic distance distributions; that is, values suggest the presence of a DNA barcode gap for a target species. Conversely, values near or equal to one give evidence for distribution overlap; that is, values likely indicate the absence of a gap.

2.2   A Bayesian Implementation

A major criticism of large sample (frequentist) theory is that it relies on asymptotic properties of the MLE (whose population parameter is assumed to be a fixed but unknown quantity), such as estimator normality and consistency. This problem is especially pronounced in the case of binomial proportions. The estimated Wald standard error (SE) of the sample proportion, is given by

$$\widehat{SE[\hat{p}]} = \sqrt{\frac{\hat{p}(1-\hat{p})}{n}}, \tag{5}$$

where $\hat{p} = \frac{Y}{n}$ is the MLE, Y is the number of successes ($Y = \sum_{i=1}^{n} y_i$) and n is the number of trials (*i.e.*, sample size). However, the above formula is problematic for several reasons. First, Equation (5) is a Normal approximation which makes use of the Central Limit Theorem (CLT); thus, large sample sizes are required for reliable estimation. When few observations are available, SEs will be large and inaccurate, leading to low statistical power to detect a true barcode gap when one sctually exists. Further, resulting interval estimates could span values less than zero or greater than one, or have zero width, which is practically meaningless. Second, when proprtions are exactly equal to zero or one, resulting SEs will be exactly zero, rendering Equation (5) completely useless. In the context of the proposed DNA barcode gap metrics, values obtained at the boundaries of their support are often encountered. Therefore, reliable calculation of SEs is not feasible. Given the importance of sufficient sampling of species genetic diversity for DNA barcoding initiatives, a different statistical estimation approach is necessary. Bayesian inference offers a natural path forward in this regard since it allows for straightforward specification of prior beliefs concerning unknown model parameters and permits the seamless propagation of uncertainty, when data is lacking and sample sizes are small, through integration with the likelihood function associated with true generating

118 processes. As a consequence, because parameters are treated as random variables, Bayesian
119 models are much more flexible and generally more easily interpretable compared to frequentist
120 approaches, since, under the latter paradigm, entire posterior distributions, along with their
121 summaries, are outputted, rather than just sampling distributions, p-values, and CIs as in
122 the former case, thus allowing direct probability statements to be made.

2.3   The Model

124 Essentially, from a statistical perspective, the goal herein is to nonparametrically estimate
125 probabilities corresponding to extreme tail quantiles for positive highly skewed distributions
126 on the unit interval (or any closed subinterval thereof). Here, it is sought to numerically
127 approximate the extent of proportional overlap/separation of intraspecific and interspecific
128 pairwise genetic distance distributions within the subinterval $[a/a', b]$. This is a challenging
129 computational problem within the current study as detailed in subsequent sections. The
130 usual approach employs Kernel Density Estimation (KDE), along with numerical or Monte
131 Carlo integration; however, this requires careful selection of the bandwidth parameter, among
132 other considerations. Here, for simplicity, a different route is taken. Counts, y, of overlapping
133 genetic distances (as expressed in the numerator of Equations (1)-(4)) are treated as
134 binomially distributed with expectation $\mathbb{E}[Y] = k\theta$, where $k = \{N, C\}$ are total count vectors
135 of intraspecific and combined genetic distances, respectively, for a target species along with
136 its nearest neighbour species, and $k = M$ is a total count vector for all pairwise species
137 comparisons. This follows from the definition of the ECDF which is binomially distributed
138 (see **Supplementary Information**). The quantity $\theta = \{p_x, q_x, p_x', q_x'\}$.
139 The metrics encompassing θ are presumed to follow a beta(α, β) distribution, with real
140 shape parameters α and β, which is a natural choice of prior on probabilities. Such a scheme
141 is quite convenient since the beta distribution is conjugate to the binomial distribution. Thus,
142 the posterior distribution is also beta distributed. Parameters were given an uninformative
143 Beta(1, 1) prior, which is equivalent to a standard uniform (Uniform(0, 1)) prior since it
144 places equal probability on all parameter values within its support. As a result, the posterior
145 is Beta($Y + 1$, $n - Y + 1$), from which various moments and other quantities, such as the
146 expected value $\mathbb{E}[Y] = \frac{Y+1}{n+2}$ and variance $\mathbb{V}[Y] = \frac{(Y+1)(n-Y+1)}{(n+2)^2(n+3)}$, can be easily calculated.
147 In general however, when possible, it is always advisable to incorporate prior information,
148 even if only weak, rather than simply imposing complete ignorance in the form of a flat prior
149 distribution. With sufficient data, the choice of prior distribution becomes less important
150 since the posterior will be dominated by the likelihood. The full univariate Bayesian model
151 for species x is thus given by

$$
\begin{aligned}
y_{\text{lwr}} &\sim \text{Binomial}(N, p_{\text{lwr}}) \\
y_{\text{upr}} &\sim \text{Binomial}(M, p_{\text{upr}}) \\
y_{\text{lwr}}' &\sim \text{Binomial}(N, p_{\text{lwr}}') \\
y_{\text{upr}}' &\sim \text{Binomial}(C, p_{\text{upr}}') \\
p_{\text{lwr}}, p_{\text{upr}}, p_{\text{lwr}}', p_{\text{upr}}' &\sim \text{Beta}(1, 1).
\end{aligned}
\tag{6}
$$

Note that p_x, q_x, $p_x^{'}$, and $q_x^{'}$ are denoted p_{lwr}, p_{upr}, $p_{\text{lwr}}^{'}$, $q_{\text{upr}}^{'}$ for distinction between MLEs and Bayesian posterior estimates.

The model, which is inherently vectorized to allow processing of multiple species datasets simultaneously, was fitted using the Stan probabilistic programming language (Carpenter et al., 2017) framework for Hamiltonian Monte Carlo (HMC) via the No-U-Turn Sampler (NUTS) sampling algorithm (Hoffman and Gelman, 2014) through the `rstan` R package (Stan Development Team, 2023). Four Markov chains were run for 2000 iterations each in parallel across four cores with random parameter initializations. Within each chain, a total of 1000 samples was discarded as warmup (*i.e.*, burnin) to reduce dependence on starting conditions. Further, 1000 post-warmup draws were utilized per chain. Because HMC/NUTS results in dependent samples that are minimally autocorrelated, chain thinning is not required. Each of these reflect default Markov Chain Monte Carlo (MCMC) settings in Stan.

Since the DNA barcode gap metrics often attain values very close to zero (suggesting no overlap and complete separation) and/or very near one (indicating no separation and complete overlap), in addition to more intermediate values, a noninformative $\text{Beta}(\frac{1}{2}, \frac{1}{2})$ prior, which is U-shaped symmetric and places greater probability density at the extremes of the distribution due to its heavier tails, while still allowing for variability in parameter estimates within intermediate values along its domain, was also attempted. However, this resulted in several divergent transitions, among other pathologies, imposed by complex geometry (*i.e.*, curvature) in the posterior space, despite remedies to resolve them, such as lowering the step size of the HMC/NUTS sampler. Note that this prior is Jeffreys' prior, which is proportional to the square root of the Fisher information and has several desirable statistical properties, most notably invariance to reparameterization.

Convergence was assessed both visually and quantitatively as follows: (1) through examining parameter traceplots, which depict the trajectory of accepted MCMC draws as a function of the number of iterations, (2) through monitoring the Gelman-Rubin $\hat{R}$ statistic (Gelman and Rubin, 1992; Vehtari et al., 2021), which measures within-chain *versus* between-chain variance, and (3) through calculating the effective sample size (ESS) for each parameter, which quantifies the number of independent samples generated Markov chains are equivalent to. Mixing of chains was deemed sufficient when traceplots looked like "fuzzy caterpillars", $\hat{R} < 1.01$, and effective sample sizes were reasonably large (Gelman et al., 2020).

A number of summary quantities were reported, including posterior means, posterior SDs, and posterior quantiles from which 95% CrIs could be computed to make probabilistic inferences concerning true population parameters.

To validate the overall correctness of the proposed statistical model given by Equation (6), in addition to generating MLEs using Equations (1)-(4) and ECDFs via R's `ecdf()` function, as a means of comparison, posterior predictive checks were also employed to generate binomial random variates in the form of counts from the posterior predictive distribution; that is $\gamma = \{Np_x, Mq_x, Np_x^{'}, Cq_x^{'}\}$ to verify that the model adequately captures relevant features of the observed data.

The proposed Bayesian model outlined herein has a straightforward interpretation (**Table 1**).

3 Case Study

4 Discussion

Supplementary Information

Information accompanying this article can be found in Supplemental Information.pdf.

Data Availability Statement

Raw data, R, and Stan code can be found on GitHub at:
https://github.com/jphill01/Bayesian-DNA-Barcode-Gap-Coalescent.

Acknowledgements

Funding

Conflict of Interest

None declared.

Author Contributions

JDP wrote the manuscript, wrote R and Stan code, approved all developed code as well as analysed and interpreted all experimental results.

References

Bergsten, J., D. Bilton, T. Fujisawa, M. Elliott, M. Monaghan, M. Balke, L. Hendrich, J. Geijer, J. Herrmann, G. Foster, I. Ribera, A. Nilsson, T. Barraclough, and A. Vogler 2012. The effect of geographical scale of sampling on DNA barcoding. *Systematic biology*, 61(5):851–869.

Carpenter, B., A. Gelman, M. Hoffman, D. Lee, B. Goodrich, M. Betancourt, M. Brubaker, J. Guo, P. Li, and A. Riddell 2017. Stan: A probabilistic programming language. *Journal of Statistical Software*, 76:1.

Gelman, A. and D. Rubin

1992. Inference from iterative simulation using multiple sequences. *Statistical Science*, 7(4):457–472.

Gelman, A., A. Vehtari, D. Simpson, C. C. Margossian, B. Carpenter, Y. Yao, L. Kennedy, J. Gabry, P.-C. Bürkner, and M. Modrák

2020. Bayesian workflow.

Hebert, P., A. Cywinska, S. Ball, and J. deWaard

2003a. Biological identifications through DNA barcodes. *Proceedings of the Royal Society of London B: Biological Sciences*, 270(1512):313–321.

Hebert, P., S. Ratnasingham, and J. de Waard

2003b. Barcoding animal life: cytochrome c oxidase subunit 1 divergences among closely related species. *Proceedings of the Royal Society of London B: Biological Sciences*, 270(Suppl 1):S96–S99.

Hebert, P. D., M. Y. Stoeckle, T. S. Zemlak, and C. M. Francis

2004. Identification of birds through dna barcodes. *PLoS Biol*, 2(10):e312.

Hoffman, M. and A. Gelman

2014. The No-U-Turn Sampler: Adaptively setting path lengths in Hamiltonian Monte Carlo. *Journal of Machine Learning Research*, 15:1593–1623.

Hubert, N. and R. Hanner

2015. DNA barcoding, species delineation and taxonomy: a historical perspective. *DNA Barcodes*, 3:44–58.

Jukes, T. and C. Cantor

1969. Evolution of protein molecules. In *Mammalian Protein Metabolism*, H. N. Munro, ed., Pp. 21–132. New York: Academic Press.

Kimura, M.

1980. A simple method for estimating evolutionary rates of base substitutions through comparative studies of nucleotide sequences. *Journal of Molecular Evolution*, 16(1):111–120.

Kingman, J.

1982. The coalescent. *Stochastic Processes and Their Applications*, 13:235–248.

Mather, N., S. Traves, and S. Ho

2019. A practical introduction to sequentially Markovian coalescent methods for estimating demographic history from genomic data. *Ecology and Evolution*, 10(1):579–589.

Meier, R., G. Zhang, and F. Ali

2008. The use of mean instead of smallest interspecific distances exaggerates the size of the "barcoding gap" and leads to misidentification. *Systematic Biology*, 57(5):809–813.

9

Meyer, C. and G. Paulay

2005. DNA barcoding: error rates based on comprehensive sampling. *PLOS Biology*, 3(12):e422.

Phillips, J., D. Gillis, and R. Hanner

2022. Lack of statistical rigor in DNA barcoding likely invalidates the presence of a true species' barcode gap. *Frontiers in Ecology and Evolution*, 10:859099.

Phillips, J., C. Griswold, R. Young, N. Hubert, and H. Hanner

2024. *A Measure of the DNA Barcode Gap for Applied and Basic Research*, Pp. 375–390. New York, NY: Springer US.

Rannala, B. and Z. Yang

2003. Bayes estimation of species divergence times and ancestral population sizes using dna sequences from multiple loci. *Genetics*, 164:1645–1656.

Ratnasingham, S. and P. Hebert

2007. BOLD: The Barcode of Life Data System (http://www. barcodinglife. org). *Molecular Ecology Notes*, 7(3):355–364.

Stan Development Team

2023. RStan: The R interface to Stan. R package version 2.21.8.

Vehtari, A., A. Gelman, D. Simpson, B. Carpenter, and P.-C. Bürkner

2021. Rank-normalization, folding, and localization: An improved $\hat{R}$ for assessing convergence of MCMC (with discussion). *Bayesian Analysis*, 16(2):667–718.

Yang, Z. and B. Rannala

2017. Bayesian species identification under the multispecies coalescent provides significant improvements to DNA barcoding analyses. *Molecular Ecology*, 26:3028–3036.
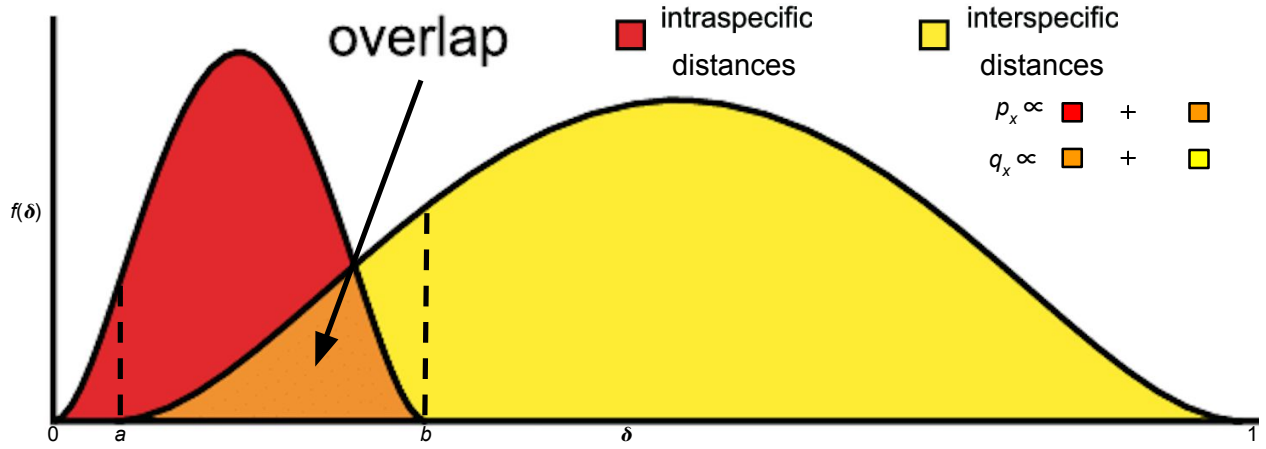
Figures and Tables

Figure 1: Modified depiction from Meyer and Paulay (2005) and Phillips et al. (2024) of the overlap/separation of pairwise intraspecific and interspecific genetic distances (δ) for calculation of the DNA barcode gap metrics (p_x and q_x) for a hypothetical species x. The minimum interspecific distance is denoted by a and the maximum intraspecific distance is indicated by b. The quantity $f(\delta)$ is akin to a kernel density estimate of the probability density function of pairwise genetic distances. A similar visualization can be displayed for p'_x and q'_x within the interval $[a', b]$.

Parameter	MLE/ECDF (95% CI)	Bayes Est. (95% CrI)
p_{lwr}		
p_{upr}		
p'_{lwr}		
p'_{upr}		

Table 2: Nonparametric frequentist and Bayesian estimates of genetic distance distribution overlap/separation for the DNA barcode gap coalescent model parameters, including 95% confidence and credible intervals.

Table 1: Interpretation of the model within $[a/a', b]$

Parameter	Explanation
p_{lwr}	When p_{lwr} is close to 0 (1), it suggests that the probability of intraspecific (interspecific) distances being larger (smaller) than interspecific (intraspecific) distances is low (high) on average, while the probability of interspecific (intraspecific) distances being larger (smaller) than intraspecific (interspecific) distances is high (low) on average; that is, there is (no) evidence for a DNA barcode gap.
p_{upr}	When p_{upr} is close to 0 (1), it suggests that the probability of interspecific (intraspecific) distances being larger (smaller) than intraspecific (interspecific) distances is high (low) on average, while the probability of intraspecific (interspecific) distances being larger (smaaler) than interspecific (intraspecfic) distances is low (high) on average; that is, there is (no) evidence for a DNA barcode gap.
p'_{lwr}	When p'_{lwr} is close to 0 (1), it suggests that the probability of intraspecific (combined interspecific distances for a target species and its nearest neighbour species) distances being larger than combined interspecific distances for a target species and its nearest neighbour species (intraspecific distances) is low (high) on average, while the probability of combined interspecific distances for a target species and its nearest neighbour species (intraspecfic distances) being larger than intraspecific distances (combined interspecific distances for a target species and its nearest neighbour species) is high (low) on average; that is, there is (no) evidence for a DNA barcode gap.
p'_{upr}	When p'_{upr} is close to 0 (1), it suggests that the probability of combined interspecific distances for a target species and its nearest neighbour species (intraspecific distances) being larger than intraspecific distances (combined interspecific distances for a target species and its nearest neighbour species) is high (low) on average, while the probability of intraspecific distances (combined interspecific distances for a target species and its nearest neighbour species) being larger than combined interspecific distances for a target species and its nearest neighbour species (intraspecific distances) is low (high) on average; that is, there is (no) evidence for a DNA barcode gap.